Dipole polarizabilities and magic wavelengths for a Sr and Yb atomic optical lattice clock

2010 J. Phys. B: At. Mol. Opt. Phys. 43 135004

(http://iopscience.iop.org/0953-4075/43/13/135004)

J. Phys. B: At. Mol. Opt. Phys. **43** (2010) 135004 (7pp) doi:10.1088/0953-4075/43/13/135004

Dipole polarizabilities and magic wavelengths for a Sr and Yb atomic optical lattice clock

Kai Guo, Guangfu Wang and Anpei Ye

Key laboratory for the Physics & Chemistry of Nanodevices, School of Electronics Engineering & Computer Science, Peking University, Beijing 100871, People's Republic of China

E-mail: yap@pku.edu.cn

Received 26 April 2010, in final form 23 May 2010
Published 22 June 2010
Online at stacks.iop.org/JPhysB/43/135004

Abstract

The magic wavelength is a crucial parameter for the optical frequency standard field. In this paper, we have calculated the dipole polarizabilities of the ground state $ns^2\,{}^1S_0$ and the metastable state $nsnp\,{}^3P_0$ for strontium and ytterbium by the method of the B-spline configuration interaction with a semiempirical core-polarization model potential, and finally obtained the values of the relevant magic wavelengths, which are 812 nm, 499 nm, and 752 nm, 550 nm, 458 nm for strontium and ytterbium atoms, respectively. The results of 812 nm and 752 nm are perfectly consistent with the corresponding experimental values. Here, we also predicted the new values of the magic wavelengths 499 nm, 550 nm and 458 nm. In addition, the relevant black-body radiation shifts, which are −1.96(37) Hz and −1.06(38) Hz for Sr and Yb, respectively, were obtained. It proves that the method we have developed is suitable to accurately calculate atomic structures of two-valence atoms, especially for their dipole polarizabilities and magic wavelengths.

The cold atom optical lattice clock represents a new generation of atomic clocks based on laser cooling technology. Its realization will improve the accuracy of the atomic clock to as low as 10^{-18} s, which is 1000 times more accurate than the Cs atomic clock. In recent years it has been found that if neutral atoms are trapped in the Lamb–Dicke regime, where the optical lattice laser works at the so-called magic wavelength [1, 2], high accuracy and stability of atomic clocks can be obtained. In the magic wavelength the ac stark shifts of both the upper and the lower levels relevant to the clock transition are equivalent; therefore, the light shift resulting from the trap laser can be eliminated.

Recently, there has been rapid development in optical lattice atomic clock research using alkaline-earth-metal atoms (also including Yb). For Sr and Yb, the transition $ns^2\,{}^1S_0$–$nsnp\,{}^3P_0$ is suitable as a clock transition. Although this transition is completely forbidden in bosonic isotopes, various schemes employing it have been proposed [3–8]. When the uncertainty of the clock transition in these schemes is estimated, the values of the dipole polarizabilities of the $ns^2\,{}^1S_0$ and $nsnp\,{}^3P_0$ states are necessary. In our previous paper [9], we calculated them and obtained the relevant magic wavelengths for group-IIB atoms (Zn, Cd and Hg). However, due to the lack of experimental values of relevant magic wavelengths, the theoretical values are just for reference. Until now, the relevant experiments have focused on ^{87}Sr and ^{174}Yb, whose experimental values of magic wavelengths have been determined to be 813.420(7) nm [10, 11] and 759.35(2) nm [12], respectively. Therefore, we can calculate them to verify our method by comparing with experimental values. In this paper, we demonstrate that our results are perfectly consistent with the experimental values. On the one hand, we can verify the previous calculations for Zn, Cd and Hg in [9], and more importantly, we can provide a widely usable approach for accurate calculation of the divalent atomic system.

As in our previous paper [9], our current work is still derived from the Dirac–Hatree–Fock calculations for the ground states of the atomic cores (Sr^{2+}, Yb^{2+}). The following calculations are all based on the HF potential of these frozen cores. It is obligatory to consider the valence correlations and the core–valence correlations in order to study the properties of strontium and ytterbium atoms. However, while the valence correlations can be accounted for completely in a configuration

interaction (CI) calculation, they are hard to assess in core–valence correlations in a similar way due to the sharply increased number of configurations. Here a semiempirical core-polarization model potential (CPMP) [13] is introduced for core–valence correlations.

During the CI calculations, B-spline states were chosen as the basis set. As a powerful numerical fitting tool, B-splines have been widely used in atomic physics, especially in many-body perturbation theory (MBPT) calculations [17, 18]. Sums over infinite bound states and integrals over continuum states can be transformed into sums over the finite B-spline states. The validity of B-spline states has been proved by various applications and successfully employed in our previous work. The calculations of dipole polarizabilities also involve sums over infinite intermediate states; thus, we use B-spline states so that these infinite sums can be approximated by finite sums without losing too many contributions from the highly exited bound states and the continuum states. To generate the relativistic B-spline states, we employed the approach of Johnson *et al* [18] but with some modifications described in our previous paper [9]. It is noteworthy that, while the large component radial wavefunctions were expanded in n B-splines of order k, the small component radial wavefunctions were expanded in $(n-1)$ B-splines of order $(k-1)$, which could eliminate the spurious state effectively [19]. Therefore in our actual calculations, 40 B-splines of order 6 and 39 B-splines of order 5 in a cavity of radius $R = 80$ au were used to expand the large and the small component radial functions, respectively.

Typically, the one-particle semiempirical core-polarization model potential can be written as

$$V_{p1}(r) = -\frac{\alpha_d}{2r^4}\left[1 - \exp\left(-\frac{r^6}{r_c^6}\right)\right], \tag{1}$$

where α_d is the polarizability of the frozen core and r_c is the cutoff radius. The values of α_d were constant throughout the computation process, while the values of r_c changed with the angular quantum number l. The values of r_c were chosen to reproduce the experimental energies for the lowest levels of each symmetry of the monovalent ions for the virtual orbitals with $l < 3$, and set equal to the geometric average of those for $l < 3$ for virtual orbitals with $l \geqslant 3$. In addition, in the calculations of the transition matrix elements, the dipole-length form in the long-wavelength approximation with the dipole operator should be accordingly modified as

$$\vec{D} = -\vec{r}\left\{1 - \frac{\alpha_d}{r^3}\left[1 - \exp\left(-\frac{r^6}{r_c^6}\right)\right]^{1/2}\right\}. \tag{2}$$

For divalent atoms such as Sr and Yb, the two-particle model potential is written as

$$V_{p2}(\vec{r_1}, \vec{r_2}) = -\alpha_d \frac{\vec{r_1}\cdot\vec{r_2}}{r_1^3 r_2^3}\left[1 - \exp\left(-\frac{r_1^6}{r_c^6}\right)\right]^{1/2} \times \left[1 - \exp\left(-\frac{r_2^6}{r_c^6}\right)\right]^{1/2}, \tag{3}$$

and the values of α_d and r_c for the Sr and Yb atoms are listed in table 1. This model potential can be introduced in the CI calculations by directly modifying the Coulomb interaction of order 1. In our CI calculations, the basis set consisted of the lowest 20 orbitals above the core shells of each symmetry of $l \leqslant 4$. The configuration numbers of the $J = 0$ and $J = 1$ states of both parities are above 1500 and 4000, respectively. Readjustment of the cutoff radii can make some calculated energies approach to the experimental values further. However, it is hard to optimize all the levels simultaneously due to the limitations of the semiempirical model itself and the effect of a reoptimization process on the reduced transition matrix elements is unpredictable. Thus, we would replace some energies with experimental values directly if necessary rather than doing any reoptimization. In fact, when CPMP is included, the results of the double-electron energy levels and transition matrix elements have greatly improved in most cases.

Table 1. Dipole polarizabilities α_d and the cutoff radii r_c of the CPMP for Sr^{2+}, Yb^{2+} (in au).

	α_d	$r_c(s_{1/2})$	$r_c(p_{1/2})$	$r_c(p_{3/2})$	$r_c(d_{3/2})$	$r_c(d_{5/2})$	$r_c(l \geqslant 3)$
Sr^{2+}	5.813[a,b]	2.022	1.949	1.951	2.200	2.207	1.761
Yb^{2+}	7.363[c]	2.143	1.695	1.643	2.185	2.232	1.962

[a] Reference [14].
[b] Reference [15].
[c] Reference [16].

Tables 2 and 3 show some low-lying energy levels of the Sr and Yb atoms, respectively. The results calculated by B-spline CI and those modified by semiempirical core-polarization model potential are both given in the tables. The effect of the modification is obvious. From the Sr atom in table 2, it is clear that the agreement between the theoretical values by B-spline CI and the experimental values is at the level of about 10%. However with reasonable modification by CPMP, the agreement improves to around 1–3%. For the Yb atom, more energy levels are listed in table 3. Similarly, the modification of CPMP makes the agreement between theoretical results and experimental values improve from around 10% to 1%. In general, we have successfully represented the energy levels of the ground state and low-lying excited states using B-spline CI. As to highly excited states, our calculation can fully represent all of the excited states using finite B-spline states.

Using the B-spline state basis set and associated CI coefficients calculated above, we obtained the reduced transition matrix elements with the dipole operator modified by CPMP (equation (2)). A few reduced dipole matrix elements between low-lying energy levels are listed in table 4. For both Sr and Yb, the corrections of CPMP improve our results towards the experimental values in most cases. The main error of reduced matrix elements by B-spline CI is derived from the lack of core–valence correlations. Since we have used semiempirical CPMP to modify the Coulomb potential and the dipole operator, all the B-spline states and associated CI coefficients can be corrected properly. As the inclusion of CPMP has contributed to an improved agreement between experimental and theoretical energies and reduced matrix elements, similarly as in [30], we estimate about 20–25% of the corrections as the final uncertainty and the final results are also listed in table 4. From our calculation and

Table 2. Low-lying energy levels of the Sr atom calculated by CI+CPMP. The values of different parities are listed separately. The experimental values are from the NIST Database [20]. Here the energy of the ground states of atomic core is chosen as zero. The last column of the table lists the differences between the results of CI+CPMP and the experimental values. All values are in au.

Configuration	CI	CI+CPMP	Experimental	Difference
		Even ($J = 0$)		
$5s5s\ ^1S_0$	−0.581 700 73	−0.616 470 38	−0.614 631 82	-1.8×10^{-3}
$5s6s\ ^1S_0$	−0.450 663 14	−0.475 551 22	−0.475 245 32	-3.1×10^{-4}
$5p5p\ ^3P_0$	−0.432 551 05	−0.460 077 84	−0.454 278 57	-5.8×10^{-3}
		Even ($J = 1$)		
$5s4d\ ^3D_1$	−0.489 581 45	−0.537 221 12	−0.531 893 07	-5.3×10^{-3}
$5s6s\ ^3S_1$	−0.458 278 01	−0.482 815 02	−0.482 321 33	-4.9×10^{-4}
$5s5d\ ^3D_1$	−0.431 766 95	−0.459 253 68	−0.455 128 45	-4.1×10^{-3}
$5p5p\ ^3P_1$	−0.430 170 54	−0.455 874 99	−0.453 336 92	-2.5×10^{-3}
		Even ($J = 2$)		
$5s4d\ ^3D_2$	−0.489 509 24	−0.536 967 39	−0.531 620 88	-5.3×10^{-3}
$5s4d\ ^1D_2$	−0.487 997 08	−0.529 854 85	−0.522 823 03	-7.0×10^{-3}
$5s5d\ ^1D_2$	−0.430 531 00	−0.459 037 69	−0.456 401 76	-2.6×10^{-3}
$5s5d\ ^3D_2$	−0.430 090 08	−0.457 888 66	−0.455 059 78	-2.8×10^{-3}
$5p5p\ ^3P_2$	−0.429 847 19	−0.455 803 96	−0.452 086 07	-3.7×10^{-3}
		Even ($J = 3$)		
$5s4d\ ^3D_3$	−0.489 350 18	−0.536 526 15	−0.531 163 10	-5.4×10^{-3}
$5s5d\ ^3D_3$	−0.430 035 85	−0.455 705 83	−0.454 954 80	-7.5×10^{-4}
		Odd ($J = 0$)		
$5s5p\ ^3P_0$	−0.526 301 57	−0.553 225 44	−0.549 396 40	-3.8×10^{-3}
$5s6p\ ^3P_0$	−0.437 276 97	−0.461 923 18	−0.460 383 84	-1.5×10^{-3}
		Odd ($J = 1$)		
$5s5p\ ^3P_1$	−0.525 538 19	−0.552 393 64	−0.548 545 13	-3.8×10^{-3}
$5s5p\ ^1P_1$	−0.487 932 37	−0.516 957 84	−0.515 766 26	-1.2×10^{-3}
		Odd ($J = 2$)		
$5s5p\ ^3P_2$	−0.523 952 86	−0.550 560 83	−0.546 748 97	-3.8×10^{-3}

our results the uncertainties of reduced dipole matrix elements could be estimated to be 3% and 5% for the Sr and Yb atoms on average. In fact, on one hand, our results of low-lying energy levels and reduced matrix elements between them have been consistent with the experimental and theoretical values; on the other hand, a few experimental values for the same reduced matrix element are sometimes quite different; hence, the experimental values of reduced matrix elements are just for reference.

For the state ψ_0, the dynamic dipole polarizability can be written as

$$\alpha_d(\omega) = 2\sum_i \frac{(E_i - E_0)}{(E_i - E_0)^2 - \omega^2} |\langle \psi_i | D_z | \psi_0 \rangle|^2, \qquad (4)$$

where E_i is the energy of a excited state $|\psi_i\rangle$, and the sum runs over all states of $\Delta J = \pm 1$ in opposite parity. Naturally, the dynamic dipole polarizability can be divided into parts α_v and α_c, which are the contributions of valence electrons and core electrons, respectively. The former could be calculated using equation (4). As to the contributions of core electrons, α_c is treated to depend on transitions of core elections from a ground state to a virtual state with energy Δ [14]. Thus α_c is written as

$$\alpha^{(c)}(\omega) = \sum_i \frac{N_i}{(\epsilon_i - \Delta)^2 - \omega^2}, \qquad (5)$$

where ϵ_i is the single-electron energy of the core shell i, N_i is the corresponding electron number and Δ is determined by fitting the static core polarizabilties listed in table 1. For the Sr and Yb atoms, Δ is −0.476 43 au and 0.512 77 au, respectively.

With these parameters and results, we calculated the dipole polarizabilities of the ground state $ns^2\ ^1S_0$ and the metastable state $nsnp\ ^3P_0$ for Sr and Yb. As the energy values of low-lying levels could directly affect the final results, and their experimental values can be very accurate, we replaced the values of a few lowest energy levels with corresponding experimental values. But as to reduced matrix elements, we did not do any replacement due to the uncertainties of their experimental values. Taking the Sr atom for example, when we calculated the values of the dipole polarizabilities of the ground state $5s^2\ ^1S_0$, the energy values of $5s^2\ ^1S_0$ and $5s5p\ ^3P_1$, $5s5p\ ^1P_1$ among more than 4000 B-spline states of against parity were replaced by their experimental values, respectively. Table 5 lists our static dipole polarizabilities for the ground state $^1S_0$ and the lowest excited state $^3P_0$ of the Sr and Yb atoms, experimental values and some other theoretical values. Clearly, our results are in good agreement with the experimental data and other literature values. In addition, dynamic dipole polarizabilities on a few selected frequencies for Sr are shown in table 6. Here we also present the dynamic dipole polarizabilities of Yb atoms in table 7.

Here we discuss the uncertainties of static dipole polarizabilities. Our calculation is based on B-spline CI. The main source of error is the fact that the B-spline method requires that the calculation be confined in a sphere at a cavity

Table 3. Low-lying energy levels of the Yb atom calculated by CI+CPMP. The values of different parities are listed separately. The experimental values are from the NIST Database [20]. Here the energy of the ground states of atomic core is chosen as zero. The last column of the table lists the differences between the results of CI+CPMP and the experimental values. All values are in au.

Configuration	CI	CI+CPMP	Experimental	Difference
		Even ($J = 0$)		
$6s6s\ ^1S_0$	−0.626 763 53	−0.680 532 40	−0.677 300 15	-3.2×10^{-3}
$6s7s\ ^1S_0$	−0.484 077 31	−0.521 444 64	−0.520 787 05	-6.6×10^{-4}
$6s8s\ ^1S_0$	−0.451 298 41	−0.490 452 23	−0.486 207 90	-4.2×10^{-3}
$6p6p\ ^3P_0$	−0.450 591 85	−0.486 143 46	−0.483 943 35	-2.2×10^{-3}
		Even ($J = 1$)		
$5d6s\ ^3D_1$	−0.510 835 64	−0.573 730 17	−0.565 719 59	-8.0×10^{-3}
$6s7s\ ^3S_1$	−0.492 151 77	−0.529 280 42	−0.528 332 17	-9.5×10^{-4}
$6s6d\ ^3D_1$	−0.459 177 69	−0.497 337 22	−0.495 918 30	-1.4×10^{-3}
$6s8s\ ^3S_1$	−0.453 043 63	−0.488 352 26	−0.487 688 10	-6.6×10^{-4}
$6p6p\ ^3P_1$	−0.446 619 42	−0.484 386 20	−0.477 707 95	-6.7×10^{-3}
$6s7d\ ^3D_1$	−0.440 451 46	−0.476 249 41	−0.475 402 65	-8.5×10^{-4}
$6s9s\ ^3S_1$	−0.437 506 35	−0.472 288 48	−0.471 712 05	-5.8×10^{-4}
$6s8d\ ^3D_1$	−0.431 324 35	−0.466 385 82	−0.465 681 35	-7.0×10^{-4}
$6s10s\ ^3S_1$	−0.429 595 95	−0.464 179 12	−0.463 712 35	-4.7×10^{-4}
$6s11s\ ^3S_1$	−0.425 486 09	−0.460 396 76	−0.459 116 35	-1.3×10^{-3}
		Even ($J = 2$)		
$5d6s\ ^3D_2$	−0.510 765 55	−0.572 637 40	−0.564 521 98	-8.1×10^{-3}
$5d6s\ ^1D_2$	−0.508 894 32	−0.562 224 95	−0.551 191 43	-1.1×10^{-2}
$6s6d\ ^3D_2$	−0.459 116 06	−0.497 252 90	−0.495 784 70	-1.5×10^{-3}
$6s6d\ ^1D_2$	−0.458 500 68	−0.496 527 89	−0.494 766 50	-1.8×10^{-3}
$6s7d\ ^3D_2$	−0.441 594 65	−0.479 994 14	−0.475 395 05	-4.6×10^{-3}
$6s7d\ ^1D_2$	−0.440 304 90	−0.476 464 03	−0.475 192 05	-1.3×10^{-3}
$6p6p\ ^3P_2$	−0.440 094 21	−0.476 031 01	−0.473 356 90	-2.7×10^{-3}
		Even ($J = 3$)		
$5d6s\ ^3D_3$	−0.510 440 28	−0.570 144 76	−0.562 157 45	-8.0×10^{-3}
$6s6d\ ^3D_3$	−0.458 836 70	−0.496 650 22	−0.495 201 25	-1.4×10^{-3}
$6s7d\ ^3D_3$	−0.440 283 75	−0.475 954 05	−0.475 086 25	-8.7×10^{-4}
$6s8d\ ^3D_3$	−0.433 838 63	−0.468 125 55	−0.465 518 75	-2.6×10^{-3}
		Odd ($J = 0$)		
$6s6p\ ^3P_0$	−0.563 011 77	−0.606 536 78	−0.598 528 23	-8.0×10^{-3}
$6s7p\ ^3P_0$	−0.469 278 31	−0.505 435 12	−0.503 746 10	-1.7×10^{-3}
$6s8p\ ^3P_0$	−0.444 464 68	−0.479 729 16	−0.478 578 90	-1.2×10^{-3}
$6s9p\ ^3P_0$	−0.433 370 37	−0.469 095 72	−0.467 334 35	-1.8×10^{-3}
		Odd ($J = 1$)		
$6s6p\ ^3P_1$	−0.560 090 05	−0.603 403 62	−0.595 322 54	-8.1×10^{-3}
$6s6p\ ^1P_1$	−0.518 368 11	−0.561 836 58	−0.563 080 93	1.2×10^{-3}
$6s7p\ ^3P_1$	−0.468 886 29	−0.505 167 88	−0.503 365 85	-1.8×10^{-3}
$6s7p\ ^1P_1$	−0.464 558 63	−0.501 784 63	−0.492 477 10	-9.3×10^{-3}
$6s8p\ ^3P_1$	−0.444 373 38	−0.479 903 00	−0.478 373 40	-1.5×10^{-3}
$6s8p\ ^1P_1$	−0.443 211 67	−0.478 814 50	−0.476 741 20	-2.1×10^{-3}
		Odd ($J = 2$)		
$6s6p\ ^3P_2$	−0.553 431 70	−0.595 744 78	−0.587 493 02	-8.3×10^{-3}
$6s7p\ ^3P_2$	−0.467 474 46	−0.503 526 28	−0.501 644 65	-1.9×10^{-3}

of finite radius, while the spatial wavefunction can extend to infinity if the principal quantum number is large enough [42]. Quantitatively speaking, according to equation (4), the static dipole polarizabilities are inversely proportional to the energy gap and proportional to the square of the corresponding reduced matrix elements. From tables 2 and 3, we can find that our results of modified low-lying energy levels have an around 1% theory–experiment disagreement on average. The energy gaps between the ground state and low-lying excited states are too small; hence the relative error could be large (10% or above). As low-lying energy levels are substituted for experimental values the uncertainties of energy gaps can be lowered to 3% or below. In addition, the uncertainties of reduced matrix elements between low-lying energy levels have been estimated to be around 3% for Sr and 5% for Yb in our previous discussion. Therefore, we can calculate that the uncertainty of static dipole polarizabilities is 6.7% for the Sr atom, while 10.9% for the Yb atom. The uncertainties have been placed in parentheses in table 5. In particular, the static dipole polarizability for $5s5p\ ^3P_0$ of Sr atoms is 409.9 au, which has 10% disagreement from other results. The reason for this is the different corrected methods. We compensate

Table 4. Reduced dipole matrix elements between part of low-lying energy levels for the Sr and Yb atoms (in au).

	CI	CI+CPMP	Final	Others	Experimental
		Sr atom			
$\|\langle 5s5p\,^3P_1\|\|d\|\|5s^2\,^1S_0\rangle\|$	0.12	0.13	0.13(1)	0.161(16)[a]	0.1555(16)[b] 0.1510(18)[c] 0.1486(17)[d]
$\|\langle 5s5p\,^1P_1\|\|d\|\|5s^2\,^1S_0\rangle\|$	5.68	5.15	5.15(15)	5.28(9)[a] 5.31[f]	5.57(6)[e] 5.40(8)[g]
$\|\langle 5s5p\,^3P_0\|\|d\|\|5s4d\,^3D_1\rangle\|$	3.30	2.53	2.53(14)		
$\|\langle 5s5p\,^3P_0\|\|d\|\|5s6s\,^3S_1\rangle\|$	1.91	1.90	1.90(1)		
		Yb atom			
$\|\langle 6s6p\,^3P_1\|\|d\|\|6s^2\,^1S_0\rangle\|$	0.40	0.41	0.41(1)	0.587[h]	
$\|\langle 6s6p\,^1P_1\|\|d\|\|6s^2\,^1S_0\rangle\|$	5.33	4.65	4.65(17)	4.825[h]	4.148(2)[i]
$\|\langle 6s6p\,^3P_0\|\|d\|\|5d6s\,^3D_1\rangle\|$	3.51	2.58	2.58(23)	2.911[h]	
$\|\langle 6s6p\,^3P_0\|\|d\|\|6s7s\,^3S_1\rangle\|$	1.89	1.83	1.83(2)	1.952[h]	

[a] Reference [21].
[b] Reference [22].
[c] Reference [23].
[d] Reference [24].
[e] Reference [25].
[f] Reference [26].
[g] Reference [27].
[h] Reference [28].
[i] Reference [29].

Table 5. Static dipole polarizabilities for the ground state $^1S_0$ and the lowest energy excited state $^3P_0$ of the Sr and Yb atoms. Some other theoretical results and experimental values are also listed (in au).

	Sr		Yb	
	$5s^2\,^1S_0$	$5s5p\,^3P_0$	$6s^2\,^1S_0$	$6s6p\,^3P_0$
Present	193(13)	410(28)	139(15)	257(28)
Experimental	186(15)[a]		142(36)[b]	
	192[c]	457.0[d]	142[e,f]	266(15)[g]
Other	194[h]	458.3(3.6)[g]	111.3(5)[g]	252(25)[j]
	197.2[d,g]		144.59[i]	302(14)[l]
			118(45)[j]	
			140.7[k]	
			141(6)[l]	

[a] Reference [31].
[b] Reference [32].
[c] Reference [33].
[d] Reference [34].
[e] Reference [35].
[f] Reference [36].
[g] Reference [37].
[h] Reference [38].
[i] Reference [39].
[j] Reference [40].
[k] Reference [41].
[l] Reference [28].

Table 6. Dynamic dipole polarizabilities and other results on a few selected frequencies for the $5s^2\,^1S_0$ and $5s5p\,^3P_0$ states of Sr. All the values are in au.

	This work		Other results[a]	
ω	$\alpha(5s^2\,^1S_0)$	$\alpha(5s5p\,^3P_0)$	$\alpha(5s^2\,^1S_0)$	$\alpha(5s5p\,^3P_0)$
0.0000	192.5	409.9	197.2	457.0
0.0499	254.4	215.7	261.2	
0.0505	256.4	220.4	263.5	
0.0560	278.1	276.5	286.0	280.5
0.0562	279.0	279.3		
0.0566	280.5	285.0	288.9	289.3
0.0652	337.2	853.0	351.8	909.2

[a] Reference [34].

Table 7. Dynamic dipole polarizabilities on a few selected frequencies for the $6s^2\,^1S_0$ and $6s6p\,^3P_0$ states of Yb. Wavelengths are in nm while other values are in au.

λ	ω	$\alpha(6s^2\,^1S_0)$	$\alpha(6s6p\,^3P_0)$
	0.0000	138.7	256.8
913.1	0.0499	169.4	69.2
902.2	0.0505	170.3	75.5
759.4	0.0600	188.5	178.6
749.4	0.0608	190.4	191.0
699.9	0.0651	201.9	306.5

for the contribution of the actual highly excited bound states and continuum states using finite B-spline states, while they choose an adjustable energy shift δ empirically as a correction.

Figure 1 shows the dynamic dipole polarizabilities of Sr atoms as a function of frequency, while figure 2 shows those of Yb atoms. In the two figures, the vertical axis represents the dynamic dipole polarizabilities of the states $ns^2\,^2S_0$ and $nsnp\,^3P_0$, while the horizontal axis stands for the frequency of the laser. The intersections in the figures give the values of the relevant magic wavelengths, which are listed in table 8. Compared with the results of the method of the Fues' model potential, the corresponding Green function (FMP+GF), the multichannel approach (FMP+MA) [43] and the results in [34], our results are closer to the experimental values.

It is worth emphasizing that for both Sr and Yb we have gained several magic wavelengths relevant to the clock

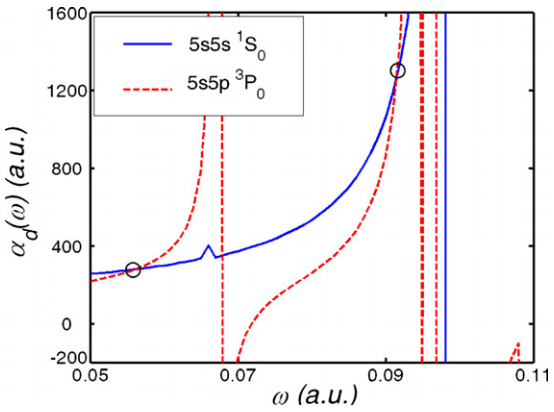

Figure 1. Dynamic dipole polarizabilities of the states $ns^2\,{}^2S_0$ and $nsnp\,{}^3P_0$ of Sr atoms as a function of frequency. The circle-marked point of intersection indicates the magic wavelength.

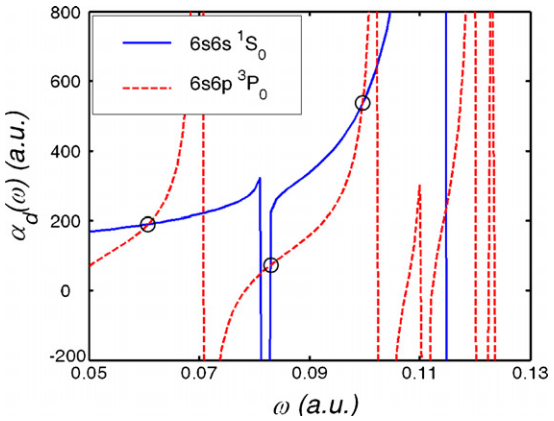

Figure 2. Dynamic dipole polarizabilities of the states $ns^2\,{}^2S_0$ and $nsnp\,{}^3P_0$ of Yb atoms as a function of frequency. The circle-marked point of intersection indicates the magic wavelength.

Table 8. Magic wavelengths of the transition $ns^2\,{}^1S_0$–$nsnp\,{}^3P_0$ for the Sr and Yb atoms (in nm).

	Present	Experimental	FMP+GF	FMP+MA	Other
Sr	812 499	813.420(7)[a,b]	800[c]		805[d]
Yb	752 550 458	759.35(2)[e]	724[c]	750[c]	759.37[f] 551.5[f] 465.4[f] 413.25[f] 402.55[f,g]

[a] Reference [10].
[b] Reference [11].
[c] Reference [43].
[d] Reference [34].
[e] Reference [12].
[f] Reference [28].
[g] unreliable.

transition $ns^2\,{}^1S_0$–$nsnp\,{}^3P_0$, while the experimental value has only one. One of them is quite consistent with the experimental values (see table 8). Moreover, during the whole calculation process, we only use a few experimental values of the lowest energy levels, which can be accurately obtained by experiment. Since our data were in good agreement with corresponding experimental values or other theoretical results, we could predict that for the Sr and Yb atoms trapped in optical lattices operated at the wavelengths around 499 nm and 550 nm, 458 nm, respectively, the null ac Stark shift could be obtained. In particular for Yb atoms, near the three points marked in figure 2 (752 nm, 550 nm, 458 nm), the shifts of the dipole polarizabilities for 6s6s $^1S_0$ are 0.2 au, 241 au and 3.2 au as the shift of the frequency is 0.0001 au, while those for 6s6p $^3P_0$ are 1.5 au, 1.4 au and 14 au, respectively. When the magic wavelength is chosen to be 550 nm, the large instabilities of dipole polarizabilities can enlarge the instabilities of the light shift and then the Allan variance can be increased; hence the stability of the atomic clock frequency can be influenced to a certain degree.

In the atomic frequency standard field, black-body radiation (BBR) shift is often the crucial factor on the ultimate uncertainty of frequency standard. It can be expressed in terms of the static polarizabilities [37, 44],

$$\delta\nu_{\mathrm{BBR}} \approx -\tfrac{2}{15}(\alpha\pi)^3 T^4 \times \left[\alpha_{^3\mathrm{P}_0}(0) - \alpha_{^1\mathrm{S}_0}(0)\right], \qquad (6)$$

where T is the temperature and α is the fine-structure constant. With our results of polarizabilities, we can find at T = 300 K, the BBR shift $\delta\nu_{\mathrm{BBR}} = -1.96(37)$ Hz for the Sr atom and $\delta\nu_{\mathrm{BBR}} = -1.06(38)$ Hz for the Yb atom, which have been calculated in [37] with the values of $-2.354(32)$ Hz and $-1.34(13)$ Hz, respectively. The differences between their results and ours are due to the differences of polarizabilities. The uncertainties of the BBR shift rest with those of relevant static dipole polarizabilities for Sr and Yb.

In summary, Sr and Yb atoms trapped in an optical lattice operated at the magic wavelengths are the best candidates for high-accuracy optical clocks. We have calculated the dipole polarizabilities of the ground state $ns^2\,{}^1S_0$ and the metastable state $nsnp\,{}^3P_0$ for the Sr and Yb atoms using the B-spline CI with a semiempirical CPMP. With these results, we obtained relevant magic wavelengths. One of these results is in good agreement with the experimental values. During our calculation procedure, we need no experimental data other than experimental energy levels and the experimental polarizability of the frozen core (α_d in table 1), which can be easily obtained. This approach would be helpful for accurate calculation of the divalent atomic system. Finally, we also estimate the values of the black-body radiation frequency shift.

Acknowledgments

The codes of this paper were run on the HP Beowulf Cluster CCSE-I (HP DL360 G4). This work was supported by the National Natural Science Foundation of China under grant no 10474003, the National Grand Fundamental Research (973 Program) of China under grant no 2005CB724501 and Instrumental Analysis Fund of Peking University.

References

[1] Ye J, Kimble H J and Katori H 2008 *Science* **320** 1734
[2] Katori H, Takamoto M, Pal'chikov V G and Ovsiannikov V D 2003 *Phys. Rev. Lett.* **91** 173005
[3] Barber Z W, Hoyt C W, Oates C W, Hollberg L, Taichenachev A V and Yudin V I 2006 *Phys. Rev. Lett.* **96** 083002
[4] Hong T, Cramer C, Nagourney W and Fortson E N 2005 *Phys. Rev. Lett.* **94** 050801
[5] Santra R, Arimondo E, Ido T, Greene C H and Ye J 2005 *Phys. Rev. Lett.* **94** 173002
[6] Taichenachev A V, Yudin V I, Oates C W, Hoyt C W, Barber Z W and Hollberg L 2006 *Phys. Rev. Lett.* **96** 083001
[7] Ovsiannikov V D, Pal'chikov V G, Taichenachev A V, Yudin V I, Katori H and Takamoto M 2007 *Phys. Rev.* A **75** 020501
[8] Yu D and Chen J 2007 *Phys. Rev. Lett.* **98** 050801
[9] Ye A and Wang G 2008 *Phys. Rev.* A **78** 014502
[10] Takamoto M, Hong F-L, Higashi R and Katori H 2005 *Nature (London)* **435** 321
[11] Takamoto M and Katori H 2003 *Phys. Rev. Lett.* **91** 223001
[12] Barber Z W *et al* 2006 *Phys. Rev. Lett.* **96** 083002
[13] Mitroy J 1993 *J. Phys. B: At. Mol. Opt. Phys.* **26** 3703
[14] Mitroy J and Bromley M W J 2003 *Phys. Rev.* A **68** 052714
[15] Johnson W R, Kolb D and Huang K 1983 *At. Data Nucl. Data Tables* **28** 333
[16] Fraga S, Karwowshi J and Saxena K M A 1976 *Handbook of Atomic Data* (Amsterdam: Elsevier)
[17] Sapirstein J and Johnson W R 1996 *J. Phys. B: At. Mol. Opt. Phys.* **29** 5213
[18] Johnson W R, Blundell S A and Sapirstein J 1988 *Phys. Rev.* A **37** 307
[19] Igarashi A 2006 *J. Phys. Soc. Jpn.* **75** 114301
[20] NIST Atomic Spectra Database[Z] http://physics.nist.gov/PhysRefData/ASD/index.html
[21] Porsev S G, Kozlov M G and Rakhlina Yu G 2000 *JETP Lett.* **72** 595
[22] Husain D and Schifino J 1984 *J. Chem. Soc. Faraday Trans.* **280** 321
[23] Drozdowski R, Ignasiuk M, Kwela J and Heldt J 1997 *Z. Phys.* D **41** 125
[24] Kelly J F, Harris M and Gallagher A 1988 *Phys. Rev.* A **37** 2354
[25] Kelly F M and Mathur M S 1980 *Can. J. Phys.* **58** 1416
[26] Porsev S G and Derevianko A 2006 *JETP* **102** 195
[27] Parkinson W H, Reeves E M and Tomkins F S 1976 *J. Phys. B: At. Mol. Phys.* **9** 157
[28] Dzuba V A and Derevianko A 2010 *J. Phys. B: At. Mol. Opt. Phys.* **43** 074011
[29] Takasu Y, Komori K, Honda K, Kumakura M, Yabuzaki T and Takahashi Y 2004 *Phys. Rev. Lett.* **93** 123202
[30] Porsev S G, Kozlov M G and Rakhlina Yu G 2001 *Phys. Rev.* A **64** 012508
[31] Miller T M and Bederson B 1976 *Phys. Rev.* A **14** 1572–3
[32] Miller T M 1996 *CRC Handbook of Chemistry and Physics* 77th edn ed D R Lide (Boca Raton, FL: CRC Press)
[33] Hyman H A 1974 *J. Chem. Phys.* **61** 4063
[34] Porsev S G, Ludlow A D, Boyd M M and Ye J 2008 *Phys. Rev.* A **78** 032508
[35] Doolen G personal communication
[36] Schwerdtfeger P 2006 *Computational Aspects of Electric Polarizability Calculations: Atoms, Molecules and Clusters* ed G Maroulis (Amsterdam: IOS)
[37] Porsev S G and Derevianko A 2006 *Phys. Rev.* A **74** 020502
[38] Sadlej A J, Urban M and Gropen O 1991 *Phys. Rev.* A **44** 5547
[39] Sahoo B K and Das B P 2008 *Phys. Rev.* A **77** 062516-1–5
[40] Porsev S G, Rakhlina Yu G and Kozlov M G 1999 *Phys. Rev.* A **60** 2781
[41] Thierfelder C and Schwerdtfeger P 2009 *Phys. Rev.* A **79** 032512
[42] Bachau H, Cormier E, Decleva P, Hansen J E and Martin F 2001 *Rep. Prog. Phys.* **64** 1815
[43] Ovsyannikov V D, Pal'chikov V G, Katori H and Takamoto M 2006 *Quantum Electron.* **36** 3
[44] Hachisu H, Miyagishi K, Porsev S G, Derevianko A, Ovsiannikov V D, Pal'chikov V G, Takamoto M and Katori H 2008 *Phys. Rev. Lett.* **100** 053001